



Semnan University



Unsteady Magnetohydrodynamic Mixed Convection Flow over a Rotating Sphere with Sinusoidal Mass Transfer

A. Sahaya Jenifer ^a, Saikrishnan Ponnaiah ^{*,a} , E. Natarajan ^b

^a Department of Mathematics, National Institute of Technology, Tiruchirappalli, India.

^b Department of Mathematics, Indian Institute of Space Science and Technology, Thiruvananthapuram, India.

PAPER INFO

Paper history:

Received: 2021-03-16

Received: 2023-01-04

Accepted: 2023-01-10

Keywords:

Boundary layer;
Heat transfer;
Variable properties;
Mixed convection;
MHD;
Non-uniform mass transfer;
Non-similar solution;
Rotating sphere.

ABSTRACT

This paper investigates the unsteady magnetohydrodynamic (MHD) mixed convective fluid flow over a rotating sphere. An implicit finite difference scheme, together with quasi-linearization, is used to find non-similar solutions for the governing equations. The impact of variable physical properties and viscous dissipation are included. It is observed that the skin friction coefficient in the axial direction and the heat transfer coefficient are increasing with an increase in MHD, mixed convection and rotation parameters and with time, whereas the effect is just the opposite for the skin friction coefficient in the rotational direction. The non-uniform slot suction(injection) and the slot movement influence the point of vanishing skin friction to move in the axial direction downstream (upstream).

DOI: [10.22075/jhmt.2023.22926.1339](https://doi.org/10.22075/jhmt.2023.22926.1339)

© 2022 Published by Semnan University Press. All rights reserved.

1. Introduction

The investigation of boundary layer flow and heat transfer over rotating bodies of revolution has several technical applications, including fiber coating, re-entry missile design, and rotary machine design [1]. The sphere being a well-renowned geometry used in engineering devices, many times the motion of spherical models endure rotation and suction/blowing. As a result, understanding the influence of rotation as well as mass transfer on flow over a spinning sphere is critical. Kreith et al. [2] have investigated convection heat transport and flow phenomena and Lee et al. [3] have incorporated forced flow over rotating spheres. The effects of surface blowing on the above-described geometry were investigated by Niazmand and Renksizbulut [4]. Recently, Safarzadeh and Brahimy [5] have established the flow phenomena over the rotating sphere in porous media. Many researchers have worked on flows over rotating bodies such as cylinders, disks, and cones, under different circumstances [6-8].

There is a substantial variation in fluid properties owing to the presence of a temperature gradient across a fluid medium. This temperature variation may be due to heat transfer when the fluid and the surface have dissimilarity in temperature or when there is a loss of heat present in the form of latent energy upon its liberation [9]. Together with these varying physical properties, the process of heat transfer for a variety of objects has already been thoughtfully analyzed by a significant number of researchers [10-16].

The mass transfer through a wall slot holds several tremendous practical implications in thermal protection, fuel injecting system of ramjets, drying theory, galvanizing the innermost section of the boundary layer in adverse pressure gradients, and reducing skin friction on high-speed aircraft [17]. Uniform suction (injection) creates discontinuities at the ends of the slot. An ultimate solution to overcome this is by implementing a non-uniform suction(injection), as discussed by Roy and Nath in [18]. Since then, several researchers have carried out the work on the impact of the non-uniform mass

*Corresponding Author: Saikrishnan Ponnaiah

Email: psai@nitt.edu

transfer over various two-dimensional axisymmetric bodies [12,13,15-17,19] and that over rotating bodies [11,14,21].

The boundary-layer flows are found to be both unsteady and non-similar in nature. The unsteadiness and non-similarity that occur may be due to the body's curvature or the velocity profiles at the boundary or the surface mass transfer, or perhaps an amalgamation of all the factors mentioned above. A vast majority of the researchers restrained their works to unsteady self-similar flows or steady non-similar flows due to mathematical complexities. A brief review of methods to find a non-similar solution for steady flows and the references of apposite works done up till 1967 has been stated in [21]. In the past two decades, many researchers worked on a non-similar solution for steady/unsteady flows over various shapes of non-spinning bodies [12,13,15,17,22-24]. In the case of rotating bodies, authors in [25-27] presented self-similar solutions for steady/unsteady flow over a rotating sphere, whereas in [10,11,28] have given non-similar solutions.

The inclusion of the effect of MHD and mixed convection has received keen attention recently. An enormous number of researchers have analyzed the effect of mixed convection on steady or unsteady fluid flow over various non-spinning bodies [17,29-32] and over rotating bodies [1,33-39]. On the other hand, the effect of MHD on steady or unsteady fluid flow over two-dimensional axisymmetric bodies has been observed by Sathyakrishna et al. [40], and over a rotating sphere has been studied in [10,27,41,42]. The above studies were focused on analyzing the flow problem with either mixed convection or magnetic field. The combined effect of MHD and mixed convection on a steady fluid flow over a sphere, rotating sphere, wedge, and the vertical elastic sheet has been studied in [11,12,19,43], respectively. Recently, Ghani and Rumite [44] have worked on the MHD mixed convection flow over a solid sphere by using the Keller-box method.

Further taking unsteadiness into account, Chamkha et al. [22,45] showed the combined effect of MHD and mixed convection of fluid flow at the forward stagnation region of a rotating sphere in the presence of chemical reaction and heat source and at different wall conditions. Mahdy et al. [26] have investigated the same with an analysis of entropy generation due to non-Newtonian Casson nanofluid. Recently, Jenifer et al. [46] obtained non-similar solutions for an unsteady MHD mixed convective flow over a stationary sphere with mass transfer. Gul et al. [47] have worked on the stagnation point flow of blood-based hybrid nanofluid over a rotating sphere with the inclusion of mixed convection and a time-dependent magnetic field. Considering an impulsively rotating sphere, Calabretto et al. [48] have explored the effects of unsteadiness and Mahdy et al. [49] have further extended the study to

homogeneous - heterogeneous reactions in MHD mixed nanofluid flow. Numerous writers have recently researched flow through spinning spheres while taking into account phenomena like double diffusive convection, magnetophoresis and joule heating. [50-52].

From the literature review, the sinusoidal mass transfer in the case of unsteady rotating sphere is not studied so far. The novelty of this work lies in finding non-similar solutions under the combined effects of the following circumstances.

- Temperature-dependent viscosity and Prandtl number
- MHD mixed convective flow over a rotating sphere
- Unsteady (accelerating) flow model
- Sinusoidal suction/injection through a slot
- Viscous dissipation and Joule heating

This study finds its applications in flows over rotating axisymmetric bodies where the flow is time dependent and the boundary layer can be controlled by implementing the above-mentioned factors. The governing equations are transformed with the help of nonsimilar transformations and the corresponding nonsimilar solutions are obtained by using implicit finite difference method along with quasilinearization technique. Important flow parameters such as skin friction and heat transfer coefficients are analyzed for various values of the effects taken into account. The fluid considered here is water due to its extreme practical applications in engineering.

2. Mathematical Formulation

The coordinate system and flow model over a heated sphere is presented in Figure 1. It is assumed that the sphere rotates with angular velocity $\Omega(t)$ (a time-dependent function) with its rotation axis parallel to $u_e(x, t)$. A constant magnetic field B_0 is enforced perpendicular to the sphere's surface. The mixed convective flow is supposed to be in the upward direction, and the sphere rotates in y -direction.

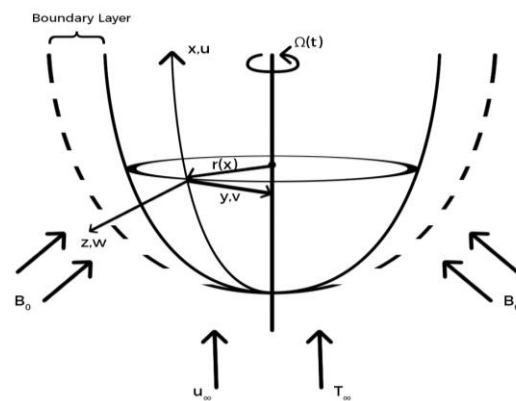


Figure 1. Flow model

The variation of temperature between the free stream and the sphere’s surface is assumed to be less than 40°C. Within this temperature limit considered, the properties of water, such as density (ρ) and specific heat (c_p) vary up to a maximum of 1%, and this minute variation allows the use of ρ and c_p as constants. On the other hand, properties such as viscosity (μ) and thermal conductivity (k) vary significantly with temperature, and so does the Prandtl number (Pr). Both μ and Pr have an inverse linear relationship with temperature as specified in [23].

$$\mu = \frac{1}{(a + bT)} \text{ and } Pr = \frac{1}{(c + dT)} \tag{1}$$

with $a = 53.41, b = 2.43, c = 0.068, d = 0.004$. (2)

The boundary layer flow is governed by the following equations:

$$(ru)_x + (rw)_z = 0 \tag{3}$$

$$u_t + uu_x + wu_z - \frac{v^2}{r}r_x = (u_e)_t + u_e(u_e)_x + \frac{1}{\rho}(\mu u_z)_z + g\beta(T - T_\infty) \sin\left(\frac{x}{R}\right) - \frac{\sigma B_0^2}{\rho}(u - u_e) \tag{4}$$

$$v_t + uv_x + wv_z + \frac{uv}{r}r_x = \frac{1}{\rho}(\mu v_z)_z - \frac{\sigma B_0^2}{\rho}v \tag{5}$$

$$T_t + uT_x + wT_z = \frac{1}{\rho} \left(\frac{\mu}{Pr} T_z \right)_z + \frac{\mu}{\rho c_p} (u_z^2 + v_z^2) + \frac{\sigma B_0^2}{\rho c_p} (u^2 + v^2 - u_e u) \tag{6}$$

Initial conditions:

$$u(x, z, 0) = u_i(x, z), \quad v(x, z, 0) = v_i(x, z), \tag{7}$$

$$w(x, z, 0) = w_i(x, z), \quad T(x, z, 0) = T_i(x, z).$$

Boundary conditions:

$$u(x, 0, t) = 0, u(x, \infty, t) = u_e(x, t), \tag{8}$$

$$v(x, 0, t) = \Omega(t)r(x), w(x, 0, t) = w_w(x, t),$$

$$T(x, 0, t) = T_w = \text{constant},$$

$$T(x, \infty, t) = T_\infty = \text{constant}.$$

The transformations to convert the equations (4)-(6) and the conditions (7) and (8) into a non-dimensional form are as follows:

$$\xi = \int_0^x \frac{U}{u_\infty} \left(\frac{x}{R}\right)^2 d\left(\frac{x}{R}\right), \bar{t} = \frac{3}{2} Re \left(\frac{\mu_e}{\rho R^2}\right) t, \tag{9}$$

$$\eta = \left(\frac{U}{u_\infty}\right) \left(\frac{Re}{2\xi}\right)^{1/2} \left(\frac{r}{R}\right) \left(\frac{z}{R}\right), Re = \frac{u_\infty R}{\nu},$$

$$\phi(\bar{t}) = 1 + \epsilon \bar{t}^2, \epsilon = 0.25, G = \frac{T - T_w}{T_\infty - T_w},$$

$$\psi(x, z, t) = u_\infty R \phi(\bar{t}) \left(\frac{2\xi}{Re}\right)^{1/2} f(\xi, \eta, \bar{t}),$$

$$\Omega = \Omega_0 \phi(\bar{t}), u = \left(\frac{R}{r}\right) \psi_z,$$

$$v = \Omega_0 r(x) \phi(\bar{t}) S(\xi, \eta, \bar{t}), w = -\left(\frac{R}{r}\right) \psi_x.$$

The above transformations satisfy (3) identically, and the non-dimensional forms of (4)-(6) are given below

$$(NF_\eta)_\eta + \phi[fF_\eta + \chi(1 - F^2)] - P[F_\bar{t} - \phi^{-1}\phi_{\bar{t}}(1 - F)] + \alpha(\xi)\phi S^2 + \phi^{-1}\lambda S_1(\xi)(1 - G) + MP(1 - F) = 2\xi\phi(F F_\xi - f_\xi F_\eta) \tag{10}$$

$$(NS_\eta)_\eta + \phi f S_\eta - P[S_\bar{t} + \phi^{-1}\phi_{\bar{t}}S] - \alpha_1(\xi)\phi FS - MPS = 2\xi\phi(F S_\xi - f_\xi S_\eta) \tag{11}$$

$$\left(\frac{1}{Pr} NG_\eta\right)_\eta + \phi f G_\eta - PG_\bar{t} + N\left(\frac{u_e}{u_\infty}\right)^2 Ec[F_\eta^2 + BS_\eta^2] + PECM\left(\frac{u_e}{u_\infty}\right)^2 \tag{12}$$

$$(F^2 + BS^2 - F) = 2\xi\phi(F G_\xi - f_\xi G_\eta)$$

with the boundary conditions

$$F(\xi, 0, \bar{t}) = 0, \quad F(\xi, \infty, \bar{t}) = 1, \tag{13}$$

$$S(\xi, 0, \bar{t}) = 1, \quad S(\xi, \infty, \bar{t}) = 0,$$

$$G(\xi, 0, \bar{t}) = 0, \quad G(\xi, \infty, \bar{t}) = 1$$

where

$$N = \frac{\mu}{\mu_\infty} = \frac{a + bT_\infty}{a + bT} = \frac{1}{E_1 + E_2 G'},$$

$$E_1 = \frac{a + bT_w}{a + bT_\infty}, E_2 = \frac{(T_\infty - T_w)b}{a + bT_\infty},$$

$$Pr = \frac{1}{c + dT} = \frac{1}{E_3 + E_4 G'}$$

$$E_3 = c + dT_w, E_4 = (T_\infty - T_w)d,$$

$$\frac{u}{u_e} = f_\eta = F, u_e = U\phi(\bar{t}),$$

$$Ec = \frac{u_\infty^2}{c_p(T_\infty - T_w)}, f = \int_0^\eta F d\eta + f_w,$$

$$\chi = \frac{2\xi dU}{U d\xi}, P = 3\xi \left(\frac{R}{r}\right)^2 \left(\frac{u_\infty}{U}\right)^2, \tag{14}$$

$$\alpha_1 = \frac{4\xi dr}{r d\xi}, M = \frac{2\sigma B_0^2 R}{3\rho\mu_\infty},$$

$$S_1(\xi) = 2\xi \left(\frac{u_\infty}{U}\right)^3 \left(\frac{R}{r}\right), \lambda = \frac{Gr}{Re^2},$$

$$Gr = \frac{g\beta\Delta T_w R^3}{\nu_\infty^2}, \nu_\infty = \frac{\mu_\infty}{\rho}, B = \left(\frac{\Omega_0 r}{U}\right)^2,$$

$$w = -\left(\frac{r}{R}\right) (2\xi Re)^{-1/2} U \phi \left[f + 2\xi f_\xi + \left(\chi + \frac{\alpha_1}{2} - 1\right) \eta F \right],$$

$$f_w = -\left(\frac{Re}{2\xi}\right)^{1/2} \phi^{-1} \int_0^x \frac{w_w(x, \bar{t})}{u_\infty} \left(\frac{r}{R}\right) d\left(\frac{x}{R}\right)$$

The velocity distribution at the boundary layer’s edge is written as,

$$\begin{aligned} \frac{u_e}{u_\infty} &= \frac{3}{2} \phi(\bar{t}) \sin \bar{x}, \quad \frac{U}{u_\infty} = \frac{3}{2} \sin \bar{x}, \\ \frac{r}{R} &= \sin \bar{x}, \quad \bar{x} = \frac{x}{R}. \end{aligned} \tag{15}$$

Hence $\xi, \beta(\xi), P(\xi), \alpha(\xi), \alpha_1(\xi), B$ and $S_1(\xi)$ can be written as expressions in \bar{x} as follows.

$$\begin{aligned} \xi &= \frac{K_1^2 K_3}{2}, \quad \chi = \frac{2K_3 K_2^{-2}}{3} \cos \bar{x}, \\ P &= \frac{2K_2^{-2} K_3}{3}, \quad \alpha = B\chi, \quad \alpha_1 = 2\chi, \\ B &= \frac{4}{9} \left(\frac{\Omega_0 R}{u_\infty} \right)^2, \quad S_1 = \frac{8K_2^{-2} K_3}{27} \end{aligned} \tag{16}$$

where

$$\begin{aligned} K_1 &= 1 - \cos \bar{x}, \quad K_2 = 1 + \cos \bar{x}, \\ K_3 &= 2 + \cos \bar{x}. \end{aligned} \tag{17}$$

The following suction/injection distribution at the wall is taken as a sinusoidal function. It exhibits a nonuniform mass transfer only in the interval $[\bar{x}_0, \bar{x}_0^*]$ which can endure a slow mass transfer at the slot's ends without breaking its continuity. Here, A is the mass transfer parameter with $A > 0$ indicating suction and $A < 0$ indicating injection through the slot. The parameter ω^* determines the slot length which is fixed at 2π whenever mass transfer is applied in this paper.

$$w_w = \begin{cases} \frac{-2Au_\infty}{(Re)^{1/2}} \sin[C(\bar{x}, \bar{x}_0)], & \bar{x} \in [\bar{x}_0, \bar{x}_0^*] \\ 0, & \text{otherwise} \end{cases} \tag{18}$$

$$C(\bar{x}, \bar{x}_0) = \omega^*(\bar{x} - \bar{x}_0).$$

The value of surface mass transfer f_w is given by

$$f_w = \begin{cases} 0, & \bar{x} \leq \bar{x}_0 \\ \frac{A}{\phi K_1} (K_3)^{-1/2} \zeta(\bar{x}, \bar{x}_0), & \bar{x} \in [\bar{x}_0, \bar{x}_0^*] \\ \frac{A}{\phi K_1} (K_3)^{-1/2} \zeta(\bar{x}_0^*, \bar{x}_0), & \text{otherwise} \end{cases} \tag{19}$$

$$\begin{aligned} \zeta(\bar{x}, \bar{x}_0) &= \frac{\sin[C(\bar{x}, \bar{x}_0) - \bar{x}] + \sin \bar{x}_0}{(\omega^* - 1)} \\ &\quad - \frac{\sin[C(\bar{x}, \bar{x}_0) - \bar{x}] - \sin \bar{x}_0}{(\omega^* + 1)}. \end{aligned}$$

It is convenient to write the equations in \bar{x} instead of ξ . \bar{x} and ξ are related by

$$\xi \frac{\partial}{\partial \xi} = Q(\bar{x}) \frac{\partial}{\partial \bar{x}} \tag{20}$$

where

$$Q(\bar{x}) = \frac{K_3 K_2^{-1}}{3} \tan \frac{\bar{x}}{2} \tag{21}$$

Substituting equations (20) and (21) in the equations (10), (11) and (12), we obtain the dimensionless equations,

$$\begin{aligned} (NF_\eta)_\eta &+ \phi[fF_\eta + \chi(1 - F^2)] \\ -P[F_{\bar{t}} - \phi^{-1}\phi_{\bar{t}}(1 - F)] &+ \alpha\phi S^2 \\ +\phi^{-1}\lambda S_1(\bar{x})(1 - G) &+ MP(1 - F) \\ = 2Q\phi(F_{F\bar{x}} - f_{\bar{x}}F_\eta) \end{aligned} \tag{22}$$

$$\begin{aligned} (NS_\eta)_\eta &+ \phi f S_\eta - P[S_{\bar{t}} + \phi^{-1}\phi_{\bar{t}}S] \\ -\alpha_1\phi FS - MPS &= 2Q\phi(FS_{\bar{x}} - f_{\bar{x}}S_\eta) \end{aligned} \tag{23}$$

$$\begin{aligned} \left(\frac{1}{Pr} NG_\eta\right)_\eta &+ \phi f G_\eta - PG_{\bar{t}} \\ +N\left(\frac{u_e}{u_\infty}\right)^2 Ec[F_\eta^2 + BS_\eta^2] \\ +PEcM\left(\frac{u_e}{u_\infty}\right)^2 (F^2 + BS^2 - F) \\ = 2Q\phi(FG_{\bar{x}} - f_{\bar{x}}G_\eta) \end{aligned} \tag{24}$$

The boundary conditions become

$$\begin{aligned} F(\bar{x}, 0, \bar{t}) &= 0, \quad F(\bar{x}, \infty, \bar{t}) = 1 \\ S(\bar{x}, 0, \bar{t}) &= 1, \quad S(\bar{x}, \infty, \bar{t}) = 0 \\ G(\bar{x}, 0, \bar{t}) &= 0, \quad G(\bar{x}, \infty, \bar{t}) = 1. \end{aligned} \tag{25}$$

The skin friction coefficients in the x – and y – directions and the heat transfer coefficient can be written as

$$\begin{aligned} C_f(Re)^{1/2} &= \frac{9K_2 K_3^{-1/2} \phi(\bar{t})}{2} \sin \bar{x} N_w(F_\eta)_w \\ \overline{C_f}(Re)^{1/2} &= \frac{9K_2 K_3^{-1/2} \phi(\bar{t})}{2} B^{1/2} \sin \bar{x} N_w(S_\eta)_w \\ Nu(Re)^{-1/2} &= \frac{3K_2 K_3^{-1/2}}{2} (G_\eta)_w \end{aligned} \tag{26}$$

where,

$$\begin{aligned} C_f &= \frac{2\left[\mu\left(\frac{\partial u}{\partial z}\right)\right]_w}{\rho u_\infty^2}, \quad \overline{C_f} = \frac{2\left[\mu\left(\frac{\partial v}{\partial z}\right)\right]_w}{\rho u_\infty^2}, \\ Nu &= \frac{R\left(\frac{\partial T}{\partial z}\right)_w}{(T_\infty - T_w)}, \\ N_w &= \frac{1}{a_1 + a_2 G_w} = \text{constant} \end{aligned} \tag{27}$$

3. Method of Solution

Quasilinearization is a technique introduced by Bellman and Kalaba [53], that can linearize nonlinear initial boundary value issues and is considered an extension of the Newton Raphson approach in functional space. This approach not only linearizes the original nonlinear equation, but it also gives a series of functions that converge to the nonlinear problem's solution. After quasilinearizing the highly nonlinear equations (22)-(24), the following set of linear partial differential equations are obtained.

$$\begin{aligned} A_1^m F_{\eta\eta}^{m+1} + A_2^m F_\eta^{m+1} + A_3^m F^{m+1} + A_4^m F_{\bar{x}}^{m+1} \\ + A_5^m G_\eta^{m+1} + A_6^m G^{m+1} + A_7^m S^{m+1} + A_8^m F_{\bar{t}}^{m+1} \\ = A_9^m \\ B_1^m S_{\eta\eta}^{m+1} + B_2^m S_\eta^{m+1} + B_3^m S^{m+1} + B_4^m S_{\bar{x}}^{m+1} \\ + B_5^m G_\eta^{m+1} + B_6^m G^{m+1} + B_7^m F^{m+1} + B_8^m S_{\bar{t}}^{m+1} \\ = B_9^m \\ C_1^m G_{\eta\eta}^{m+1} + C_2^m G_\eta^{m+1} + C_3^m G^{m+1} + C_4^m G_{\bar{x}}^{m+1} \\ + C_5^m F_\eta^{m+1} + C_6^m F^{m+1} + C_7^m S_\eta^{m+1} + C_8^m S^{m+1} \\ + C_9^m G_{\bar{t}}^{m+1} = C_{10}^m \end{aligned} \tag{28}$$

Here, the superscript m and $m + 1$ denote the previous and current iterations and the coefficients are as follows

$$\begin{aligned} A_1 &= N \\ A_2 &= \phi f + 2Q\phi f_{\bar{x}} - E_2 N^2 G_\eta \\ A_3 &= -2\phi\chi F - P\phi^{-1}\phi_{\bar{t}} - MP - 2Q\phi F_{\bar{x}} \\ A_4 &= -2Q\phi F \\ A_5 &= -E_2 N^2 F_\eta \\ A_6 &= -\phi^{-1}\lambda S_1 + 2E_2^2 N^3 F_\eta G_\eta - E_2 N^2 F_{\eta\eta} \\ A_7 &= 2\alpha\phi S \\ A_8 &= -P \\ A_9 &= -\phi\chi(1 + F^2) - P\phi^{-1}\phi_{\bar{t}} + \alpha\phi S^2 - MP \\ &\quad - 2Q\phi F F_{\bar{x}} - E_2 N^2 F_\eta G_\eta + 2E_2^2 N^3 F_\eta G_\eta G \\ &\quad - E_2 N^2 F_{\eta\eta} G - \phi^{-1}\lambda S_1 \end{aligned}$$

$$\begin{aligned} B_1 &= N \\ B_2 &= \phi f + 2Q\phi f_{\bar{x}} - E_2 N^2 G_\eta \\ B_3 &= -P\phi^{-1}\phi_{\bar{t}} - \alpha_1\phi F - MP \\ B_4 &= -2Q\phi F \\ B_5 &= -E_2 N^2 S_\eta \\ B_6 &= 2E_2^2 N^3 S_\eta G_\eta - E_2 N^2 S_{\eta\eta} \\ B_7 &= -\alpha_1\phi S - 2Q\phi S_{\bar{x}} \\ B_8 &= -P \\ B_9 &= -\alpha_1\phi S F - 2Q\phi F S_{\bar{x}} - E_2 N^2 S_\eta G_\eta \\ &\quad + 2E_2^2 N^3 S_\eta G_\eta G - E_2 N^2 S_{\eta\eta} G \end{aligned}$$

$$\begin{aligned} C_1 &= \frac{N}{Pr} \\ C_2 &= \phi f + 2Q\phi f_{\bar{x}} + 2\left(E_4 N - \frac{E_2 N^2}{Pr}\right) G_\eta \\ C_3 &= -E_2 N^2 Ec \left(\frac{u_e}{u_\infty}\right)^2 (F_\eta^2 + BS_\eta^2) \\ &\quad + 2\left(-E_2 E_4 N^2 + \frac{E_2^2 N^3}{Pr}\right) G_\eta^2 + \left(E_4 N - \frac{E_2 N^2}{Pr}\right) G_{\eta\eta} \\ C_4 &= -2Q\phi F \\ C_5 &= 2NEc \left(\frac{u_e}{u_\infty}\right)^2 F_\eta \\ C_6 &= PEcM \left(\frac{u_e}{u_\infty}\right)^2 (2F - 1) - 2Q\phi G_{\bar{x}} \\ C_7 &= 2NEc \left(\frac{u_e}{u_\infty}\right)^2 BS_\eta \\ C_8 &= 2PEcM \left(\frac{u_e}{u_\infty}\right)^2 BS \\ C_9 &= -P \\ C_{10} &= G_\eta^2 \left(E_4 N - \frac{E_2 N^2}{Pr}\right) + C_3 G - 2Q\phi F G_{\bar{x}} \\ &\quad + NEc \left(\frac{u_e}{u_\infty}\right)^2 (F_\eta^2 + BS_\eta^2) + PEcM \left(\frac{u_e}{u_\infty}\right)^2 (F^2 + BS^2) \end{aligned}$$

All the coefficients above are known values from m -th iteration. With step sizes $\Delta\eta, \Delta\bar{x}, \Delta\bar{t}$ in their respective directions, the linearized partial differential equations in (28) are discretized using central difference scheme in η direction and backward difference scheme in \bar{x}, \bar{t} directions and the linear difference equations are written in the following matrix form [54]

$$X_{i,j,k}\zeta_{i,j-1,k} + Y_{i,j,k}\zeta_{i,j,k} + Z_{i,j,k}\zeta_{i,j+1,k} = W_{i,j,k}, \quad (29)$$

$$2 \leq j \leq \bar{J}$$

where the coefficient matrices are as follows

$$X_j = \begin{bmatrix} A_1 - A_2 \frac{\Delta\eta}{2} & 0 & -A_5 \frac{\Delta\eta}{2} \\ 0 & B_1 - B_2 \frac{\Delta\eta}{2} & -B_5 \frac{\Delta\eta}{2} \\ -C_5 \frac{\Delta\eta}{2} & -C_7 \frac{\Delta\eta}{2} & C_1 - C_2 \frac{\Delta\eta}{2} \end{bmatrix}$$

$$Y_j = \begin{bmatrix} -2A_1 + H_1\Delta\eta^2 & A_7\Delta\eta^2 & A_6\Delta\eta^2 \\ B_7\Delta\eta^2 & -2B_1 + H_2\Delta\eta^2 & B_6\Delta\eta^2 \\ C_6\Delta\eta^2 & C_8\Delta\eta^2 & -2C_1 + H_3\Delta\eta^2 \end{bmatrix}$$

$$Z_j = \begin{bmatrix} A_1 + A_2 \frac{\Delta\eta}{2} & 0 & A_5 \frac{\Delta\eta}{2} \\ 0 & B_1 + B_2 \frac{\Delta\eta}{2} & B_5 \frac{\Delta\eta}{2} \\ C_5 \frac{\Delta\eta}{2} & C_7 \frac{\Delta\eta}{2} & C_1 + C_2 \frac{\Delta\eta}{2} \end{bmatrix}$$

$$W_j = \begin{bmatrix} \left(A_9 + \frac{A_4}{\Delta\bar{x}} F_{i-1,j,k} + \frac{A_8}{\Delta\bar{t}} F_{i,j,k-1}\right) \Delta\eta^2 \\ \left(B_9 + \frac{B_4}{\Delta\bar{x}} S_{i-1,j,k} + \frac{B_8}{\Delta\bar{t}} S_{i,j,k-1}\right) \Delta\eta^2 \\ \left(C_{10} + \frac{C_4}{\Delta\bar{x}} G_{i-1,j,k} + \frac{C_9}{\Delta\bar{t}} G_{i,j,k-1}\right) \Delta\eta^2 \end{bmatrix}$$

$$\zeta_{i,j,k} = \begin{bmatrix} F_{i,j,k} \\ S_{i,j,k} \\ G_{i,j,k} \end{bmatrix}$$

where

$$H_1 = A_3 + \frac{A_4}{\Delta\bar{x}} + \frac{A_8}{\Delta\bar{t}}, H_2 = B_3 + \frac{B_4}{\Delta\bar{x}} + \frac{B_8}{\Delta\bar{t}}$$

$$H_3 = C_3 + \frac{C_4}{\Delta\bar{x}} + \frac{C_9}{\Delta\bar{t}}.$$

The system of tridiagonal blocks (29) is then solved by using Varga's algorithm [55] for ζ in η direction, which is discretized into \bar{J} subintervals, with fixed \bar{x}, \bar{t} and the forward marching continues in \bar{x} direction. The above-mentioned process repeats for the subsequent steps in \bar{t} direction.

The convergence of the solution at each step is assumed to be achieved when the maximum absolute difference between the current and previous iterations is less than the tolerance value, which is set at 10^{-4} . Here, the step sizes are taken as $\Delta\eta = 10^{-2}, \Delta\bar{x} = 5 \times 10^{-4}$ and $\Delta\bar{t} = 10^{-2}$. η_∞ is considered to be 6.

4. Results and Discussion

The precision of our study is ensured by comparing the obtained solutions with those available in the literature in both steady and unsteady cases.

In the case of steady flow, the effect of rotation B on the skin friction parameters $[(F_\eta)_w, -(S_\eta)_w]$ and the heat transfer parameter, $[(G_\eta)_w]$ are presented in Figure 2, and the effect of mixed convection parameter λ on skin friction coefficient in x -direction $[C_f(Re)^{1/2}]$ is shown in Figure 3.

The results are compared with those of Roy and Saikrishnan [14] and Chen et al. [29], respectively.

Also, in the case of unsteady flow, the impact of MHD parameter M on $C_f(Re)^{1/2}$ at times $\bar{t} = 0, 2$ are presented in Figure 4 and are compared with those of Sathyakrishna et al. [40]. All the above-mentioned studies agree with our results.

The variations in the skin friction coefficients in the x, y -directions and the heat transfer coefficient $[C_f(Re)^{1/2}, \bar{C}_f(Re)^{1/2}, Nu(Re)^{-1/2}]$ at various streamwise locations due to the MHD parameter M with $T_\infty = 18.7^\circ\text{C}, \Delta T_w = 10^\circ\text{C}, B = 1, \lambda = 20, A = 0, Ec = 0$ are presented in Figure 5 and Figure 6 for both steady and unsteady cases. From the figures, $C_f(Re)^{1/2}$ enhances from zero, hits maximum value and then declines as \bar{x} increases. With an increase in M and \bar{t} , both $C_f(Re)^{1/2}$ and $Nu(Re)^{-1/2}$ increase, whereas the effect is just the opposite on $\bar{C}_f(Re)^{1/2}$. The reason for this is the magnetic field B_0 induces a magnetic force which in turn creates a supporting force in the meridian direction and an opposing force in the rotational direction. Hence, increasing M accelerates the flow in x -direction and decelerates the flow in y -direction and thus resulting in the enhancement of $C_f(Re)^{1/2}, Nu(Re)^{-1/2}$ and reduction in $\bar{C}_f(Re)^{1/2}$. For fixed $M, Nu(Re)^{-1/2}$ decreases monotonically as \bar{x} increases. In the case of steady flow, the significance of the MHD parameter is not pronounced on $C_f(Re)^{1/2}$ and $Nu(Re)^{-1/2}$. However, the effect becomes significant with time \bar{t} .

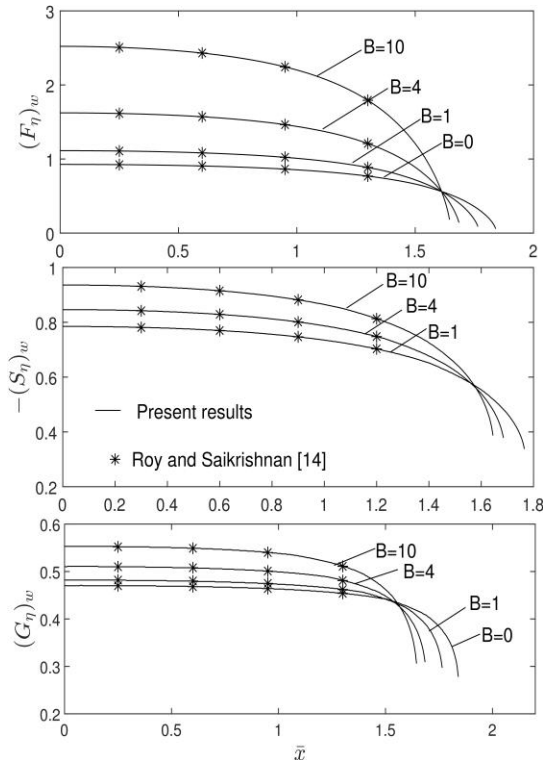


Figure 2. Comparison of the velocity profiles in x, y -directions and temperature profile for a steady flow with those of Roy and Saikrishnan [14] where $T_\infty = 18.7^\circ\text{C}, \Delta T_w = 20^\circ\text{C}$, constant viscosity and Prandtl number

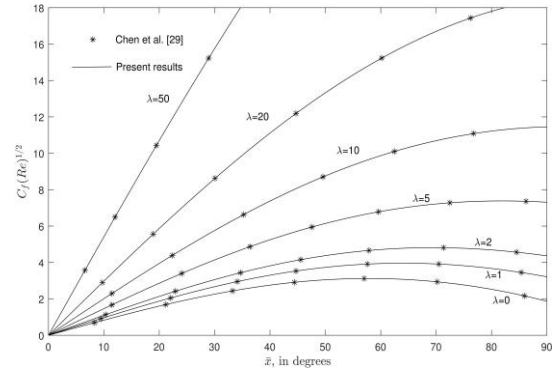


Figure 3. Comparison of the skin friction parameter in the x -direction with those of Chen et al. [29] where $T_\infty = 18.7^\circ\text{C}, \Delta T_w = 10^\circ\text{C}$, constant viscosity and Prandtl number

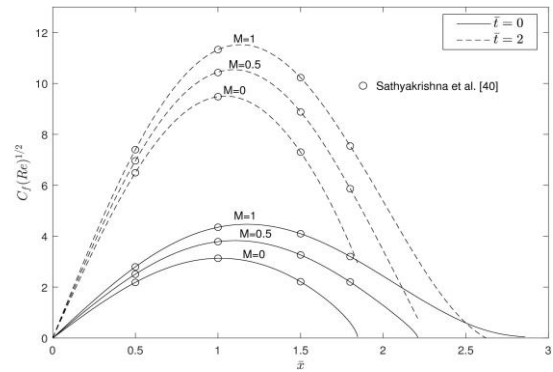


Figure 4. Comparison of the skin friction parameter in the x -direction for an unsteady flow with those of Sathyakrishna et al. [40] where $T_\infty = 18.7^\circ\text{C}, \Delta T_w = 10^\circ\text{C}$

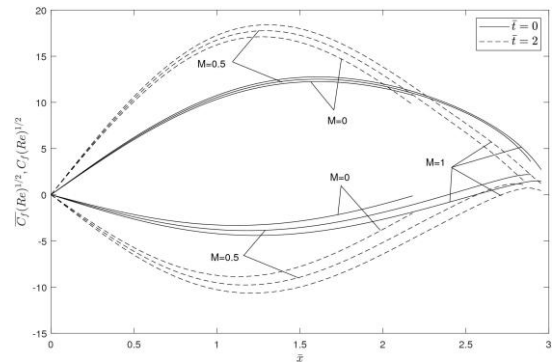


Figure 5. Effect of the MHD parameter M on the skin friction coefficients in x, y -directions for $\lambda = 20, B = 1$

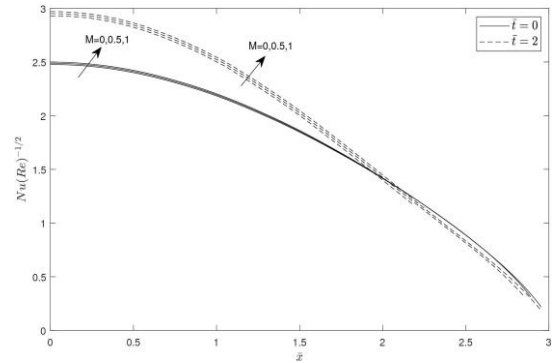


Figure 6. Effect of the MHD parameter M on the heat transfer coefficient for $\lambda = 20, B = 1$

Figure 7 and Figure 8 depict the influence of the mixed convection parameter λ on $C_f(Re)^{1/2}$, $\overline{C_f}(Re)^{1/2}$ and $Nu(Re)^{-1/2}$ over time for $T_\infty = 18.7^\circ\text{C}$, $\Delta T_w = 10^\circ\text{C}$, $B = 1, M = 1, A = 0, Ec = 0$. The presence of mixed convection parameter $\lambda \neq 0$ signifies favorable pressure gradient. This results in thinning of momentum and temperature boundary layers. As a consequence, both $C_f(Re)^{1/2}$ and $Nu(Re)^{-1/2}$ increase and $\overline{C_f}(Re)^{1/2}$ decreases as λ increases at both times $\bar{t} = 0, 2$. It is to be noted that the significance of λ is more prominent on $C_f(Re)^{1/2}$ than on $\overline{C_f}(Re)^{1/2}$ because there is no explicit dependence of the mixed convection parameter λ in equation (23).

Figure 9 and Figure 10 show the impact of rotation parameter B on $C_f(Re)^{1/2}$, $\overline{C_f}(Re)^{1/2}$ and $Nu(Re)^{-1/2}$ for $T_\infty = 18.7^\circ\text{C}$, $\Delta T_w = 10^\circ\text{C}$, $M = 1, \lambda = 10, A = 0, Ec = 0$. It is found that increasing rotation parameter B results in an increase of $C_f(Re)^{1/2}$ and $Nu(Re)^{-1/2}$ and decrease of $\overline{C_f}(Re)^{1/2}$ at both $\bar{t} = 0$ and 2. This is because the fluid entering in the axial direction has been forced outward in the rotational direction due to the centrifugal force and has been replaced by the cooler fluid from the normal direction. This results in accelerating the fluid flow in the axial direction and contracting the thickness of momentum boundary layer in that direction as well as the thickness of the thermal boundary layer. Meanwhile, in the rotational direction, the momentum boundary layer thickens. Also, the effect of B on $Nu(Re)^{-1/2}$ is found to be small since B affects it indirectly.

For the steady flow, $\overline{C_f}(Re)^{1/2}$ vanishes while $C_f(Re)^{1/2}$ does not. As B increases, the point of vanishing skin friction coefficient in y -direction moves slightly downwards, indicating an ordinary separation. It is also observed that $C_f(Re)^{1/2}$ vanishes for $B > 0, \bar{t} > 0$, and the point of vanishing skin friction in that direction moves upstream as B increases. However, this does not imply separation since it is unsteady.

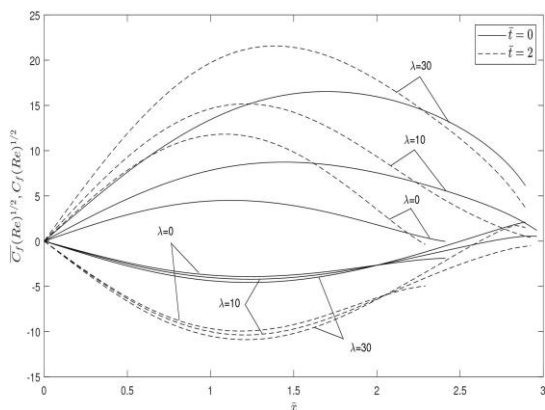


Figure 7. Effect of the mixed convection parameter λ on the skin friction coefficients in x, y -directions for $M = 1, B = 1$

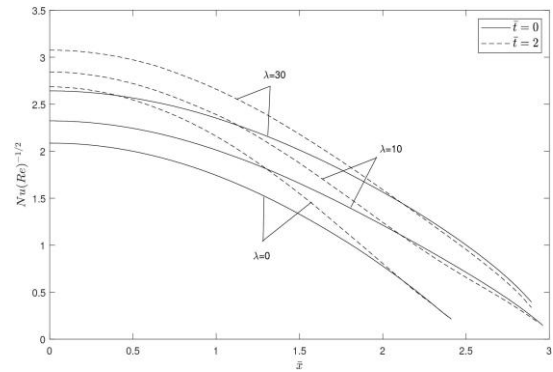


Figure 8. Effect of the mixed convection parameter λ on the heat transfer coefficient for $M = 1, B = 1$

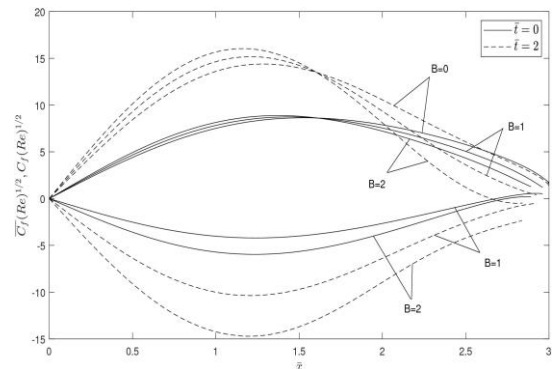


Figure 9. Effect of the rotation parameter B on the skin friction coefficients in x, y -directions for $M = 1, \lambda = 10$

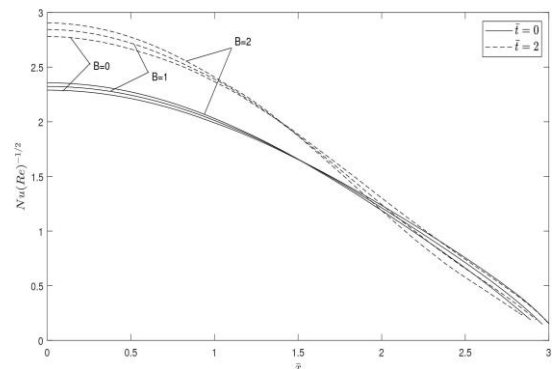


Figure 10. Effect of the rotation parameter B on the heat transfer coefficient for $M = 1, \lambda = 10$

The impact of the viscous dissipation parameter Ec on $Nu(Re)^{-1/2}$ for $A = 0, M = 1, \lambda = 2, B = 1$ has been shown in Figure 11. The heat transfer coefficient $Nu(Re)^{-1/2}$ decreases for the change of values of Ec from 0 to -0.1 in both steady and unsteady cases. At $\bar{x} = 1.5$, the percentage decrease of $Nu(Re)^{-1/2}$ is 129% when $\bar{t} = 0$ and 413% at $\bar{t} = 2$ as Ec changes from 0 to -0.1 . Also, the occurrence of negative $Nu(Re)^{-1/2}$ is physically simulated by the reversal of heat transfer direction.

The reason for this can be seen from the temperature profile G at $\bar{x} = 1.5$ depicted in Figure 12. For $Ec \neq 0$ and $\bar{t} = 2$, the temperature G gets below zero near the wall. This is because nonzero Ec emphasizes the presence of the viscous dissipation and M too being nonzero brings on joule heating in the

energy equation. Due to the impact of these two heating, the fluid near the wall heats up and its temperature becomes more than T_w , although originally T_w was higher. This results in the wall being heated up instead of being cooled and hence the heat transfer reversal observed in Figure 11. However, such a phenomenon is not observed in the steady case. Ec does not show much of a difference in the skin friction coefficients in x, y –directions as well as the velocity profiles. Hence, the corresponding figures are omitted in this paper.

Figures 13-16 show the influence of non-uniform mass transfer on $C_f(Re)^{1/2}$, $\overline{C_f}(Re)^{1/2}$ and $Nu(Re)^{-1/2}$ for $\lambda = 0.5, B = 1$ and $M = 0.5$, at $\bar{t} = 0$ and $\bar{t} = 2$. The effect of suction/injection is examined through two slots $[\bar{x}_0, \bar{x}_0^*]$, one at $[0.5, 1]$ and the other at $[1.25, 1.75]A > 0$), as the slot starts, $C_f(Re)^{1/2}$ and $Nu(Re)^{-1/2}$ increase and hit their maximum before the slot's end. Contrastingly, $\overline{C_f}(Re)^{1/2}$ decreases as the slot starts and hits its minimum before the slot's end. As the suction parameter increases, the fluid at the sphere's surface, which has low velocity, is sucked through the slot $[\bar{x}_0, \bar{x}_0^*]$ and is replaced by the fluid in the subsequent layers with comparatively higher velocity. This augments the velocity gradients in both x and y –directions at the wall ($F_\eta, -S_\eta$)_w and thus resulting in increasing $C_f(Re)^{1/2}$ and decreasing $\overline{C_f}(Re)^{1/2}$.

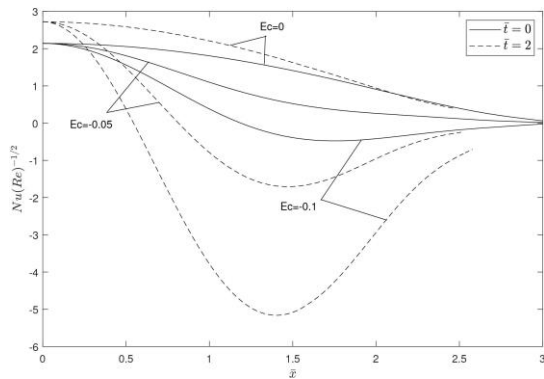


Figure 11. Effect of the viscous dissipation parameter Ec on the heat transfer coefficient for $\lambda = 2, M = 1, B = 1$

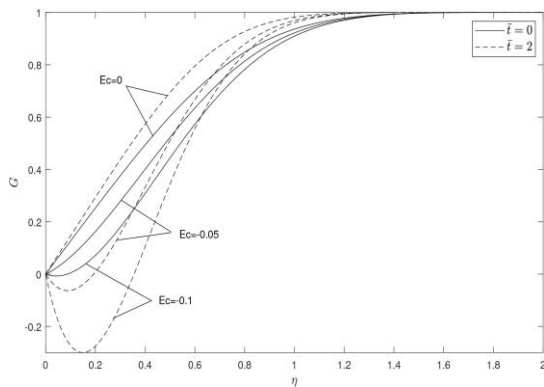


Figure 12. Effect of the viscous dissipation parameter Ec on the temperature profile at $\bar{x} = 1.5$ for $\lambda = 2, M = 1, B = 1$

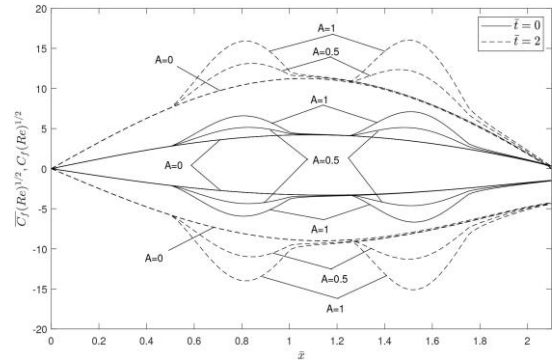


Figure 13. Effect of the non-uniform slot suction A on the skin friction coefficients in x, y –directions for $\lambda = 0.5, M = 0.5, B = 1$, slots at $\bar{x}_0 = 0.5, 1.25$

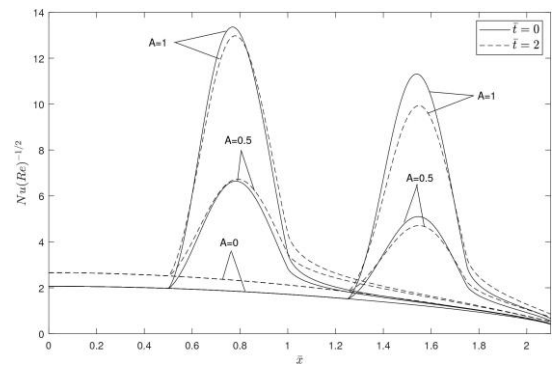


Figure 14. Effect of the non-uniform slot suction A on the heat transfer coefficient for $\lambda = 0.5, M = 0.5, B = 1$, slots at $\bar{x}_0 = 0.5, 1.25$

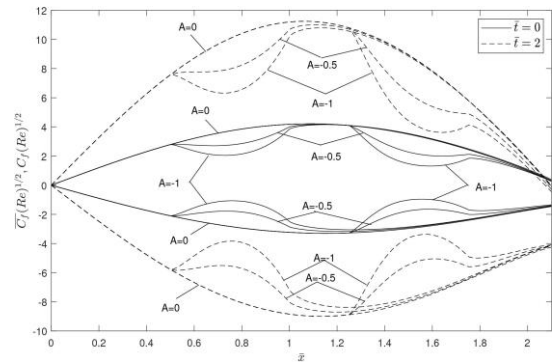


Figure 15. Effect of the non-uniform slot injection A on the skin friction coefficients in x, y –directions for $\lambda = 0.5, M = 0.5, B = 1$, slots at $\bar{x}_0 = 0.5, 1.25$

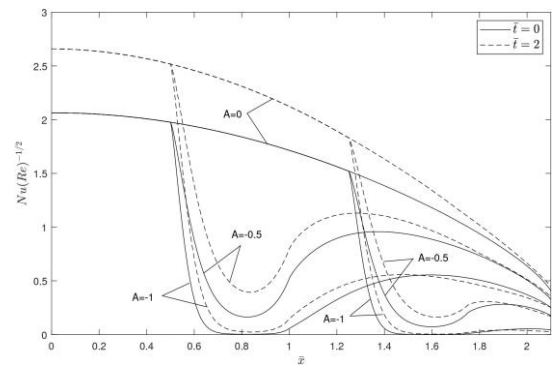


Figure 16. Effect of the non-uniform slot injection A on the heat transfer coefficient for $\lambda = 0.5, M = 0.5, B = 1$, slots at $\bar{x}_0 = 0.5, 1.25$

Moreover, since the fluid being sucked is warmer than the adjacent layers, the more the suction, the steeper the temperature gradient at the wall and hence $Nu(Re)^{-1/2}$ is enhanced.

The slot injection's ($A < 0$) effect on skin friction and heat transfer coefficients is qualitatively opposite to that of suction in the slot region. In all the above cases, regardless of A , the coefficients $[C_f(Re)^{1/2}, -\overline{C}_f(Re)^{1/2}, Nu(Re)^{-1/2}]$ are enhanced as \bar{t} increases and the impact is more pronounced in the unsteady case, since the flow is accelerating with \bar{t} . For the steady case ($\bar{t} = 0$), the suction/injection doesn't impact the zero skin frictions in both directions. However, when $\bar{t} > 0$, the point of zero skin friction in x -direction moves downstream with an increase in suction parameter ($A > 0$). The slot movement in the downstream direction from $[0.5,1]$ to $[1.25,1.75]$ helps the vanishing point of $C_f(Re)^{1/2}$ move further downstream. Meanwhile, the opposite effect is seen with an enhancement in the injection parameter. It should be emphasized here that zero skin friction in only one direction/both directions does not imply the ordinary/singular separation as the flow considered here is unsteady.

Conclusion

An unsteady MHD mixed convection boundary layer flow problem over a geometry of rotating sphere has been solved numerically, and the observations are as follows.

- The MHD parameter (M) affects the skin friction coefficient in x -direction and heat transfer coefficient noticeably in the unsteady case than it does in the steady case for fixed non-zero values of rotation and mixed convection parameters.
- The mixed convection parameter (λ) is found to have a prominent effect on the skin friction coefficient in the x -direction and the heat transfer coefficient in the y -direction, in both steady and unsteady cases.
- For non-zero values of rotation parameter B , an ordinary separation is noted in the steady case as $\overline{C}_f(Re)^{1/2}$ vanishes while $C_f(Re)^{1/2}$ does not. It is observed that $C_f(Re)^{1/2}$ vanishes for $B > 0$, $\bar{t} > 0$, and that point of vanishing moves upstream as the rotation parameter increases.
- At both times $\bar{t} = 0$ and 2 , the more the magnitude of viscous dissipation parameter (Ec) the less the heat transfer coefficient as a result of heating due to viscous and joule heating effects. Moreover, the unsteadiness results in drastic decrement in the heat transfer coefficient as dissipation increases.
- The temperature drops below zero in the vicinity of the sphere's surface in the unsteady case, indicating the fluid near the surface of the sphere getting warmer instead of colder.

- For fixed non-zero values of B, M, λ and $\bar{t} > 0$, non-uniform slot suction or slot movement helps the vanishing skin friction in x -direction to move slightly downstream, whereas the injection shows the opposite effect.

Nomenclature

A	Dimensionless mass transfer parameter
B_0	Magnetic field strength (T)
B	Dimensionless rotation parameter
c_p	Specific heat at constant pressure ($kJ \cdot kg^{-1} \cdot K^{-1}$)
C_f	Skin friction coefficient in the x -direction
\overline{C}_f	Skin friction coefficient in the y -direction
Ec	Eckert number (viscous dissipation parameter)
f	Dimensionless stream function
f_w	Surface mass transfer distribution
F	Dimensionless velocity component in the x -direction
g	Gravity ($m \cdot s^{-2}$)
G	Dimensionless temperature
Gr	Grashof number
k	Thermal conductivity ($W \cdot m^{-1} \cdot K^{-1}$)
M	MHD parameter
N	μ/μ_∞ Viscosity ratio
Nu	Nusselt number
Pr	Prandtl number
r	Radius of the section normal to the axis of the sphere (m)
R	Radius of the sphere (m)
Re	Reynolds number
S	Dimensionless velocity component in the y -direction
t	Dimensional time (s)
\bar{t}	Dimensionless time
T	Temperature (K)
u, v, w	Dimensional velocity components in x, y, z -directions, respectively ($m \cdot s^{-1}$)
U	Steady state velocity at the boundary layer's edge ($m \cdot s^{-1}$)
x, y, z	Dimensional meridional, azimuthal and normal distances, respectively (m)
\bar{x}	Dimensionless meridional distance
\bar{x}_0, \bar{x}_0^*	Ends of slot
Greek Symbols	
χ	Dimensionless pressure gradient
β	Volumetric coefficient of thermal expansion (K^{-1})
$\Delta\eta, \Delta\bar{x}, \Delta\bar{t}$	Step sizes in η, \bar{x} - and \bar{t} -directions, respectively
η, ξ	Transformed coordinates
ϵ	Constant used in the continuous function of time
λ	Mixed convection parameter
μ	Dynamic viscosity ($kg \cdot m^{-1} \cdot s^{-1}$)

ν	Kinematic viscosity ($m^2 \cdot s^{-1}$)
ρ	Density ($kg \cdot m^{-3}$)
σ	Electrical conduction ($\Omega^{-1} \cdot m^{-1}$)
ψ	Dimensional stream function ($m^2 \cdot s^{-1}$)
$\phi(\bar{t})$	Continuous function of time
Ω	Angular velocity ($rad \cdot s^{-1}$)
ω^*	Slot length parameter

Subscripts

e	Conditions at the edge of boundary layer
w	Conditions at the surface of the sphere
∞	Conditions in the free stream
x, z, \bar{x}	Partial derivatives with respect to these variables
\bar{t}, ξ, η	

Acknowledgements

The authors are thankful to the reviewers for their valuable comments. The first author would like to thank National Institute of Technology Tiruchirappalli for supporting through an institute fellowship.

References

- [1] Lien, F.S., Chen, C.K. and Cleaver, J.W., 1986. Mixed and Free Convection Over a Rotating Sphere with Blowing and Suction. *Journal of Heat Transfer*, 108(2), pp.398–404.
- [2] Kreith, F., Roberts, L.G., Sullivan, J.A. and Sinha, S.N., 1963. Convection Heat Transfer and Flow Phenomena of Rotating Spheres. *International Journal of Heat and Mass Transfer*, 6(10), pp.881–895.
- [3] Lee, M.H., Jeng, D.R. and De Witt, K.J., 1978. Laminar Boundary Layer Transfer Over Rotating Bodies in Forced Flow. *Transactions of the ASME*, 100, pp.496–502.
- [4] Niazmand, H. and Renksizbulut, M., 2005. Flow Past a Spinning Sphere with Surface Blowing and Heat Transfer. *Journal of Fluids Engineering*, 127(1), pp.163–171.
- [5] Safarzadeh, S. and Brahimi, A., 2022. Convection Heat Transfer and Flow Phenomena from a Rotating Sphere in Porous Media. *Scientia Iranica*, 29(2), pp.588–596.
- [6] Attia, H.A., 2009. Steady Flow Over a Rotating Disk in Porous Medium with Heat Transfer. *Nonlinear Analysis: Modelling and Control*, 14(1), pp.21–26.
- [7] Al-Maliky, R.F., 2013. Numerical Investigation of Laminar Flow Over a Rotating Circular Cylinder. *International Journal of Mechanical & Mechatronics Engineering*, 13(3), pp.32–44.
- [8] Towers, P.D. and Garrett, S.J., 2016. Similarity Solutions of Compressible Flow Over a Rotating Cone with Surface Suction. *Thermal Science*, 20(2), pp.517–528.
- [9] Schlichting, H. and Gersten, K., 2016. *Boundary-Layer Theory*, Springer.
- [10] Mahdy, A., 2018. Simultaneous Impacts of MHD and Variable Wall Temperature on Transient Mixed Casson Nanofluid Flow in the Stagnation Point of Rotating Sphere. *Applied Mathematics and Mechanics*, 39(9), pp.1327–1340.
- [11] Rajakumar, J., Saikrishnan, P. and Chamkha, A., 2016. Non-similar Solution of Steady MHD Mixed Convection Flow Over a Rotating Sphere. *Computational Thermal Sciences*, 8(6), pp.509–523.
- [12] Rajakumar, J., Saikrishnan, P. and Chamkha, A., 2016. Non-uniform Mass Transfer in MHD Mixed Convection Flow of Water Over a Sphere with Variable Viscosity and Prandtl Number. *International Journal of Numerical Methods for Heat & Fluid Flow*, 26(7), pp.2235–2251.
- [13] Revathi, G., Saikrishnan, P. and Chamkha, A., 2013. Non-similar Solution for Unsteady Water Boundary Layer Flows Over a Sphere with Non-uniform Mass Transfer. *International Journal of Numerical Methods for Heat & Fluid Flow*, 23(6), pp.1104–1116.
- [14] Roy, S. and Saikrishnan, P., 2003. Non-Uniform Slot Injection (Suction) Into Steady Laminar Water Boundary Layer Flow Over a Rotating Sphere. *International Journal of Heat and Mass Transfer*, 46(18), pp.3389–3396.
- [15] Saikrishnan, P. and Roy, S., 2002. Steady Nonsimilar Axisymmetric Water Boundary Layers with Variable Viscosity and Prandtl Number. *Acta Mechanica*, 157(1–4), pp.187–199.
- [16] Saikrishnan, P. and Roy, S., 2003. Non-uniform Slot Injection (Suction) Into Water Boundary Layers Over (i) a Cylinder and (ii) a Sphere. *International Journal of Engineering Science*, 41(12), pp.1351–1365.
- [17] Ganapathirao, M., Ravindran, R. and Pop, I., 2013. Non-uniform Slot Suction (Injection) on an Unsteady Mixed Convection Flow Over a Wedge with Chemical Reaction and Heat Generation or Absorption. *International Journal of Heat and Mass Transfer*, 67, pp.1054–1061.
- [18] Roy, S. and Nath, G., 1994. Non-uniform Slot Injection (Suction) or Wall Enthalpy into a Steady Nonsimilar Compressible Laminar Boundary Layer. *Acta Mechanica*, 103, pp.45–61.
- [19] Ganapathirao, M. and Ravindran, R., 2015. Non-uniform Slot Suction/Injection Into Mixed Convective MHD Flow Over a Vertical Wedge with Chemical Reaction. *Procedia Engineering*, 127, pp.1102–1109.
- [20] Subhashini, S.V., Takhar, H.S. and Nath, G., 2007. Non-uniform Mass Transfer or Wall Enthalpy Into a Compressible Flow Over a Rotating Sphere. *Heat and Mass Transfer*, 43(11), pp.1133–1141.
- [21] Dewey, C.F. and Gross, J.F., 1967. Exact Similar Solutions of the Laminar Boundary-Layer

- Equations, *Advances in Heat Transfer*, Elsevier, 4, pp.317–446.
- [22] Chamkha, A.J. and Ahmed, S.E., 2012. Unsteady MHD Heat and Mass Transfer by Mixed Convection Flow in the Forward Stagnation Region of a Rotating Sphere at Different Wall Conditions. *Chemical Engineering Communications*, 199(1), pp.122–141.
- [23] Eswara, A.T. and Nath, G., 1994. Unsteady Nonsimilar Two-Dimensional and Axisymmetric Water Boundary Layers with Variable Viscosity and Prandtl Number. *International Journal of Engineering Science*, 32(2), pp.267–279.
- [24] Roy, S., Takhar, H.S. and Nath, G., 2004. Unsteady MHD Flow on a Rotating Cone in a Rotating Fluid. *Meccanica*, 39(3), pp.271–283.
- [25] Anilkumar, D. and Roy, S., 2004. Self-Similar Solution of the Unsteady Mixed Convection Flow in the Stagnation Point Region of a Rotating Sphere. *Heat and Mass Transfer*, 40(6), pp.487–493.
- [26] Mahdy, A., Chamkha, A.J. and Nabwey, H.A., 2020. Entropy Analysis and Unsteady MHD Mixed Convection Stagnation-Point Flow of Casson Nanofluid Around a Rotating Sphere. *Alexandria Engineering Journal*, 59(3), pp.1693–1703.
- [27] Takhar, H.S. and Nath, G., 2000. Self-Similar Solution of the Unsteady Flow in the Stagnation Point Region of a Rotating Sphere with a Magnetic Field. *Heat and Mass Transfer*, 36(2), pp.89–96.
- [28] Sau, A., 1994. Unsteady Non-similar Compressible Boundary Layer Flow over a Rotating Sphere. *Acta Mechanica*, 106(3–4), pp.207–213.
- [29] Chen, T.S. and Mucoglu, A., 1977. Analysis of Mixed Forced and Free Convection About a Sphere. *International Journal of Heat and Mass Transfer*, 20(8), pp.867–875.
- [30] Devi, C.D.S. and Nath, G., 1988. Unsteady Mixed Convection Over Two-Dimensional and Axisymmetric Bodies. *Wärme- Und Stoffübertragung*, 22(1–2), pp.83–90.
- [31] Natarajan, E., Basak, T. and Roy, S., 2008. Natural Convection Flows in a Trapezoidal Enclosure With Uniform and Non-Uniform Heating of Bottom Wall. *International Journal of Heat and Mass Transfer*, 51(3–4), pp.747–756.
- [32] Natarajan, E., Basak, T. and Roy, S., 2007. Natural Convection in a Trapezoidal Cavity With Linearly Heated Side Wall (s). In *Heat Transfer Summer Conference*, 42746 pp. 1021–1030.
- [33] Hatem, N., Philippe, C., Mbow, C., Kabdi, Z., Najoua, S. and Daguene, M., 1996. Numerical Study of Mixed Convection Around a Sphere Rotating About Its Vertical Axis in a Newtonian Fluid at Rest and Subject to a Heat Flux. *Numerical Heat Transfer, Part A: Applications*, 29(4), pp.397–415.
- [34] Hatzikonstantinou, P., 1990. Effects of Mixed Convection and Viscous Dissipation on Heat Transfer about a Porous Rotating Sphere. *ZAMM - Journal of Applied Mathematics and Mechanics*, 70(10), pp.457–463.
- [35] Le Palec, G. and Daguene, M., 1987. Laminar Three-Dimensional Mixed Convection About a Rotating Sphere in a Stream. *International Journal of Heat and Mass Transfer*, 30(7), pp.1511–1523.
- [36] Rajasekaran, R. and Palekar, M.G., 1985. Mixed Convection About a Rotating Sphere. *International Journal of Heat and Mass Transfer*, 28(5), pp.959–968.
- [37] Rajasekaran, R. and Palekar, M.G., 1985. Viscous Dissipation Effects on Mixed Convection About a Rotating Sphere. *International Journal of Engineering Science*, 23(8), pp.789–795.
- [38] Tieng, S.M. and Yan, A.C., 1992. Investigation of Mixed Convection About a Rotating Sphere by Holographic Interferometry. *Journal of Thermophysics and Heat Transfer*, 6(4), pp.727–732.
- [39] Patil, P.M., Benawadi, S. and Shanker, B., 2022. Influence of Mixed Convection Nanofluid Flow over a Rotating Sphere in the Presence of Diffusion of Liquid Hydrogen and Ammonia. *Mathematics and Computers in Simulation*, 194, pp.764–781.
- [40] Sathyakrishna, M., Roy, S. and Nath, G., 2001. Unsteady Two-Dimensional and Axisymmetric MHD Boundary-Layer Flows. *Acta Mechanica*, 150(1–2), pp.67–77.
- [41] Turkyilmazoglu, M., 2011. Numerical and Analytical Solutions for the Flow and Heat Transfer near the Equator of an MHD Boundary Layer over a Porous Rotating Sphere. *International Journal of Thermal Sciences*, 50(5), pp.831–842.
- [42] Kazem, S., Tameh, M.S. and Rashidi, M.M., 2019. An Improvement To The Unsteady MHD Rotating Flow Over a Rotating Sphere Near the Equator via Two Radial Basis Function Schemes. *The European Physical Journal Plus*, 134(12), p.611.
- [43] Vajravelu, K., Li, R., Dewasurendra, M. and Prasad, K.V., 2017. Mixed Convective Boundary Layer MHD Flow Along a Vertical Elastic Sheet. *International Journal of Applied and Computational Mathematics*, 3(3), pp.2501–2518.
- [44] Ghani, M. and Rumite, W., 2021. Keller-Box Scheme to Mixed Convection Flow over a Solid Sphere with the Effect of MHD. *MUST: Journal of Mathematics Education, Science and Technology*, 6(1), pp.97–120.
- [45] Chamkha, A.J. and Ahmed, S.E., 2011. Unsteady MHD Heat and Mass Transfer by Mixed Convection Flow in the Forward Stagnation Region of a Rotating Sphere in the Presence of Chemical Reaction and Heat Source. In

- Proceedings of the World Congress on Engineering, 1 pp.133–138.
- [46] Sahaya Jenifer, A., Saikrishnan, P. and Lewis, R.W., 2021. Unsteady MHD Mixed Convection Flow of Water over a Sphere with Mass Transfer. *Journal of Applied and Computational Mechanics*, 7(2), pp.935–942.
- [47] Gul, T., Ali, B., Alghamdi, W., Nasir, S., Saeed, A., Kumam, P., Mukhtar, S., Kumam, W. and Jawad, M., 2021. Mixed Convection Stagnation Point Flow of the Blood Based Hybrid Nanofluid around a Rotating Sphere. *Scientific Reports*, 11(1), pp.1–15.
- [48] Calabretto, S.A., Levy, B., Denier, J.P. and Mattner, T.W., 2015. The Unsteady Flow Due to an Impulsively Rotated Sphere, *Proceedings of the Royal Society A: Mathematical, Physical and Engineering Sciences*, 471(2181), p.20150299.
- [49] Mahdy, A.E.N., Hady, F.M. and Nabwey, H.A., 2021. Unsteady Homogeneous-Heterogeneous Reactions in MHD Nanofluid Mixed Convection Flow Past a Stagnation Point of an Impulsively Rotating Sphere. *Thermal Science*, 25(1 Part A), pp.243–256.
- [50] Almakki, M., Mondal, H., Mburu, Z. and Sibanda, P., 2022. Entropy Generation in Double Diffusive Convective Magnetic Nanofluid Flow in Rotating Sphere with Viscous Dissipation. *Journal of Nanofluids*, 11(3), pp.360–372.
- [51] Das, K., Kundu, P.K. and Sk, M.T., 2022. Magnetophoretic Effect on the Nanofluid Flow Over Decelerating Spinning Sphere with the Presence of induced Magnetic Field. *Journal of Nanofluids*, 11(1), pp.135–141.
- [52] Mahmood, Z., Alhazmi, S.E., Khan, U., Bani-Fwaz, M.Z. and Galal, A.M., 2022. Unsteady MHD Stagnation Point Flow of Ternary Hybrid Nanofluid over a Spinning Sphere with Joule Heating. *International Journal of Modern Physics B*, 36(32), p.2250230.
- [53] Bellman, R.E. and Kalaba, R.E., 1965. *Quasilinearization and Nonlinear Boundary Value Problems*, The RAND Corporation, American Elsevier Publishing Company, Inc., New York.
- [54] Inouye, K. and Tate, A., 1974. Finite-Difference Version of Quasi-Linearization Applied to Boundary-Layer Equations. *AIAA Journal*, 12(4), pp.558–560.
- [55] Varga, S., 2000. *Matrix Iterative Analysis*, Springer-Verlag Berlin Heidelberg.